10. Mechanism of Transfer of a Basic Drug across the Water/1,2-Dichloroethane Interface: the Case of Quinidine

by **Frédéric Reymond**[a]), **Guillaume Steyaert**[b]), **Pierre-Alain Carrupt**[b]), **Bernard Testa**[b]), and **Hubert H. Girault**[a])*

[a]) Laboratoire d'Electrochimie, Ecole Polytechnique Fédérale de Lausanne, CH–1015 Lausanne
[b]) Institut de Chimie Thérapeutique, Section de Pharmacie, Université de Lausanne, CH–1015 Lausanne

(24.X.95)

The electrochemical transfer of quinidine across the H_2O/1,2-dichloroethane interface was investigated by cyclic voltammetry, so as to determine its lipophilicity. The formal transfer potential was measured as a function of the pH of the aqueous phase. Both singly and doubly protonated quinidine cations can transfer across the interface, and their formal *Gibbs* free energies of transfer were observed to be 7.7 and 31.2 kJ mol^{-1}, respectively. Between pH 0 and 3, only the doubly charged quinidine was present in the aqueous phase and was observed to transfer. Between pH 3 and 6, the transfer of both cations occurred. The proportion of doubly charged quinidine decreased progressively in this pH range and disappeared completely above pH 6. The overall process was analyzed using a thermodynamic model. The relationship between the various forms of quinidine in both phases and pH was established and found to be in good agreement with the experimental results. With this model, the acid-base equilibrium constants in the organic phase could be calculated as $pK_{a1o} = 9.66 \pm 0.21$ and $pK_{a2o} = 14.20 \pm 0.16$ (the subscripts a1o and a2o refer to the first and second dissociation constants). This study illustrates how the partition of ionic species can be taken into account in the determination of lipophilicity and in the description of the passive transfer of organic drugs.

1. Introduction. – In recent years, much interest has focused on the experimental investigation and theoretical determination of electrochemical processes at the interface between two immiscible electrolyte solutions (ITIES) [1–4]. This is due to the wide range of applications these systems have found in chemistry and biology [5–10].

The interface between an organic and a water phase has been frequently inferred as a simple model of biological membranes. Therefore, studies on drug transfer characteristics and mechanisms in such systems are of great importance not only for the fundamental understanding of liquid/liquid interfaces, but also for a better comprehension of *in vivo* drug disposition. In pharmacological terms, one can distinguish between two types of drug transfer across biological membranes [11–13]: first, the active (*i.e.* carrier-mediated) transport of ionized compounds such as inorganic ions and amino acids, which controls the transport of charged and polar endogenous molecules (*e.g.* ion channels for K^+, Na^+, and Ca^{2+}), and second, passive transfer, which is controlled by diffusion and related to molecular size and lipophilicity. In electrochemistry, only ions are considered, where this passive transfer simply means the partition across an interface, mediated by a potential-driven process.

In medicinal chemistry, very little is known on the passive transfer of organic ions, *e.g.* ionized drugs. Here, the accepted hypothesis is that such compounds cross membranes only in their neutral form or as ion pairs. However, recent studies suggest a significant passive transfer of organic ions [12] [14–16], which should be taken into account to overcome the limitations of common models describing the disposition of drugs.

This paper addresses the transfer mechanism of the dibasic drug quinidine across the H_2O/1,2-dichloroethane (CH_2ClCH_2Cl) interface as a function of pH. Cyclic voltammetry at the large ITIES was used to study the transfer characteristics of the different ionic forms of quinidine, and a thermodynamic model was established to describe the passive transfer of this drug.

2. Theory. – 2.1. *Preliminary Remarks.* Quinidine is an organic anti-arrhythmic drug, the structure of which [17] [18] is shown in *Fig. 1.*

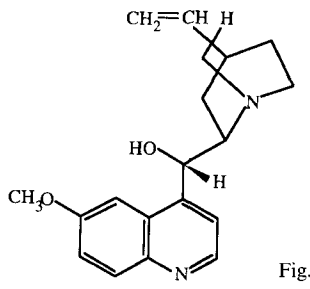

Fig. 1. *Structure of quinidine (Q)*

The solubility of neutral quinidine (Q) is very low in aqueous solution, but it can form soluble singly protonated (QH^+) or doubly protonated (QH_2^{2+}) species in acidic solution, as described by the following protonation equilibria:

$$QH_2^{2+} \underset{k_2}{\overset{k_1}{\rightleftarrows}} QH^+ + H^+ \text{ and } QH^+ \underset{k_4}{\overset{k_3}{\rightleftarrows}} Q + H^+$$

K_{a1w} and K_{a2w}, the first and second dissociation constants of quinidine in H_2O, are given by *Eqn. 1* where a_i represent the activities of the species i in the respective phases.

$$K_{a1w} = \frac{a^w_{QH^+} a^w_{H^+}}{a^w_{QH_2^{2+}}} \quad \text{and} \quad K_{a2w} = \frac{a^w_{Q} a^w_{H^+}}{a^w_{QH^+}} \tag{1}$$

2.2. *Thermodynamic Model.* The transfer of both QH_2^{2+} and QH^+ from H_2O into the organic phase may occur when an electrical potential difference is applied across the interface. This modifies the acid-base equilibria in the vicinity of the interface. Thus, upon transfer of a species (*e.g.* QH_2^{2+} from H_2O to the organic phase), a concentration gradient is established along which QH_2^{2+} molecules may diffuse from the bulk or which facilitates the production of QH_2^{2+} by protonation of QH^+ at the interface. The distribution of species in solution, therefore, depends on both protonation equilibria and also on the potential applied across the interface.

Considering that analogous protonation equilibria can also be established in the organic phase and that all the charged species may transfer from one phase to the other, depending on the interfacial potential difference, the transfer process of quinidine can be expressed as shown in *Fig. 2.*

In the vicinity of the interface, all acid-base equilibria are perturbed when a potential is applied. This, in turn, establishes a reaction layer on both sides of the interface.

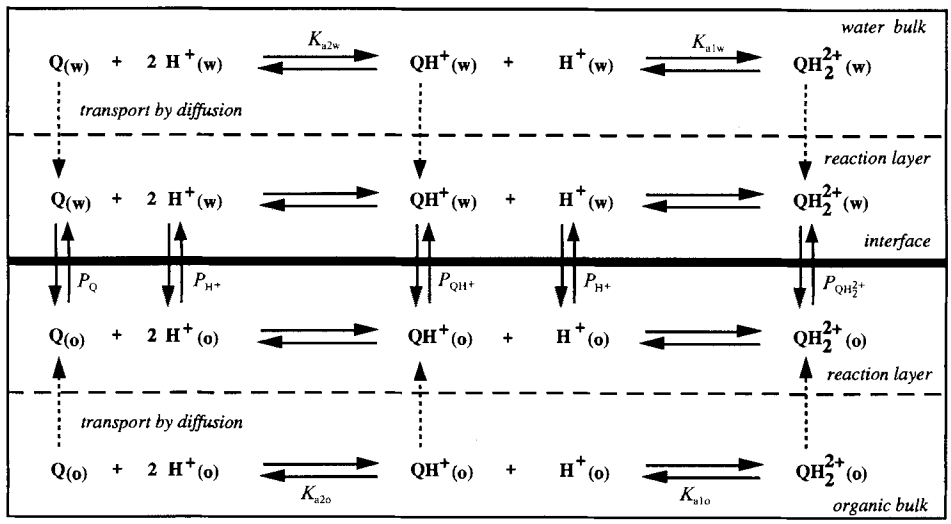

Fig. 2. *Thermodynamic equilibria for the transfer of the various ionic forms of quinidine.* K_{a1w}, K_{a2w}, K_{a1o}, and K_{a2o} represent the first and second dissociation constants in the water and the organic phases, respectively. P_Q, P_{QH^+}, $P_{QH_2^{2+}}$, and P_{H^+} are the partition coefficients between the two phases for neutral, singly charged, and doubly charged quinidine and protons, respectively.

However, the bulk of each phase remains unchanged on the very short experimental time scale, and both dissociation equilibria are maintained during a potential sweep.

For reversible ion transfer controlled by diffusion at the interface, the partition of the ionized form of a species may be described by the *Nernst* equation for the ITIES [4], *i.e. Eqn. 2*, where $\Delta^{w}_{o}\phi$ is the applied *Galvani* potential difference between the organic (o) and the aqueous (w) phase ($\phi^w - \phi^o$), and c_i^o and c_i^w are the concentrations in the organic and water phases, respectively. $\Delta^{w}_{o}\phi_i^{o'}$ is the formal ion transfer potential of the ionic species i related to the standard transfer potential $\Delta^{w}_{o}\phi_i^{o}$ by *Eqn. 3* where γ_i are the activity coefficients of the species i.

$$\Delta^{w}_{o}\phi = \Delta^{w}_{o}\phi_i^{o'} + \frac{RT}{z_i F}\ln\left(\frac{c_i^o}{c_i^w}\right) \tag{2}$$

$$\Delta^{w}_{o}\phi_i^{o'} = \Delta^{w}_{o}\phi_i^{o} + \frac{RT}{z_i F}\ln\left(\frac{\gamma_i^o}{\gamma_i^w}\right) \tag{3}$$

Likewise, the standard *Gibbs* free energy of transfer is given by *Eqn. 4* [4], and by analogy we can define a formal *Gibbs* energy of transfer by *Eqns. 5*.

$$\Delta G^{o,w\to o}_{tr,i} = z_i F \Delta^{w}_{o}\phi_i^{o} = \mu_i^{o,o} - \mu_i^{o,w} \tag{4}$$

$$\Delta G^{o',w\to o}_{tr,i} = z_i F \Delta^{w}_{o}\phi_i^{o'} = \mu_i^{o,o} - \mu_i^{o,w} + \frac{RT}{z_i F}\ln\left(\frac{\gamma_i^o}{\gamma_i^w}\right) \tag{5}$$

It is important to notice that the standard *Gibbs* energy of transfer refers to the transfer from pure H_2O to pure organic solvent. It is, therefore, different from the *Gibbs* energy of partition, which refers to the transfer from H_2O saturated with organic solvent

to organic solvent saturated with H_2O. Nevertheless, in the case of solvents of low miscibility such as H_2O/CH_2ClCH_2Cl, the ionic standard *Gibbs* free energy of transfer is often equal to the ionic standard *Gibbs* free energy of partition [6]. Consequently, both terms will be used without differentiation in this paper.

In this manner, the activities of all the species present can be described by the set of *Eqns. 6–12* which includes the partition coefficients, the dissociation equilibria given in *Eqn. 1*, and the electrochemical equilibria given by *Eqn. 2*. The partitioning of the neutral quinidine is described by *Eqn. 6*.

$$\ln P_Q = \ln\left(\frac{a_Q^o}{a_Q^w}\right) = -\frac{\Delta G_{tr,Q}^{o,w\to o}}{RT} \tag{6}$$

Contrary to the partition of neutral species such as molecules or salts for which the partition coefficient is a unique quantity related to the standard *Gibbs* energy of transfer of the species, the partition of ionic species is potential-dependent as shown by *Eqn. 2*. For the protonated form of the quinidine, *Eqns. 7–10* hold.

$$\ln P_{QH^+} = \ln\left(\frac{a_{QH^+}^o}{a_{QH^+}^w}\right) = \frac{F(\Delta_o^w\phi - \Delta_o^w\phi_{QH^+}^o)}{RT} = \frac{F\Delta_o^w\phi}{RT} - \frac{\Delta G_{tr,QH^+}^{o,w\to o}}{RT} \tag{7}$$

or

$$\ln P_{QH^+} = \ln P_{QH^+}^o + \frac{F\Delta_o^w\phi}{RT} \tag{8}$$

$$\ln P_{QH_2^{2+}} = \ln\left(\frac{a_{QH_2^{2+}}^o}{a_{QH_2^{2+}}^w}\right) = \frac{2F(\Delta_o^w\phi - \Delta_o^w\phi_{QH_2^{2+}}^o)}{RT} = \frac{2F\Delta_o^w\phi}{RT} - \frac{\Delta G_{tr,QH_2^{2+}}^{o,w\to o}}{RT} \tag{9}$$

or

$$\ln P_{QH_2^{2+}} = \ln P_{QH_2^{2+}}^o + \frac{2F\Delta_o^w\phi}{RT} \tag{10}$$

Similarly for the proton, *Eqns. 11* or *12* have to be considered.

$$\ln P_{H^+} = \ln\left(\frac{a_{H^+}^o}{a_{H^+}^w}\right) = \frac{F(\Delta_o^w\phi - \Delta_o^w\phi_{H^+}^o)}{RT} = \frac{F\Delta_o^w\phi}{RT} - \frac{\Delta G_{tr,H^+}^{o,w\to o}}{RT} \tag{11}$$

or

$$\ln P_{H^+} = \ln P_{H^+}^o + \frac{F\Delta_o^w\phi}{RT} \tag{12}$$

For these equations, P^o represent the standard partition coefficient of the ions, *i.e.* the partition coefficient when the interface is not polarized. Finally, to calculate the different concentrations, we can consider for simplicity a system where the two phases are of equal volume for which we can express the law of conservation of mass by *Eqn. 13*.

$$c_Q^w + c_{QH^+}^w + c_{QH_2^{2+}}^w + c_Q^o + c_{QH^+}^o + c_{QH_2^{2+}}^o = c_{Q\,total} \tag{13}$$

c_{total} is the total amount of all quinidine species present in both phases. It is set to the value of 1 in all calculations and thus used as a normalization parameter. The different formal potentials for reaction transfer can be determined by cyclic voltammetry from the measurement of the half-wave potentials for the respective ion-transfer reactions.

This model represents a new and more thorough method to determine the thermodynamic equilibria in – and between – both phases, since it does not neglect the partitioning of the ionic species or of the proton into the organic phase.

2.3. *Theoretical Concentration Profiles.* The above system can be solved as a function of proton activity in the water phase, a^{w}_{H+}, and of the applied *Galvani* potential. The solution is given by *Eqns. 14–21*:

$$c^{w}_{Q} = \frac{K_{a1w} K_{a2w} c_{Q\,total}}{A} \gamma^{o}_{Q} \gamma^{w}_{QH+} \gamma^{w}_{QH_2^{2+}} \tag{14}$$

$$c^{w}_{QH+} = \frac{K_{a1w} c_{Q\,total} a^{w}_{H+}}{A} \gamma^{o}_{Q} \gamma^{w}_{Q} \gamma^{w}_{QH_2^{2+}} \tag{15}$$

$$c^{w}_{QH_2^{2+}} = \frac{c_{Q\,total} [a^{w}_{H+}]^2}{A} \gamma^{w}_{QH+} \gamma^{o}_{Q} \gamma^{w}_{Q} \tag{16}$$

$$c^{o}_{Q} = \frac{P_Q K_{a1w} K_{a2w} c_{Q\,total}}{A} \gamma^{w}_{Q} \gamma^{w}_{QH+} \gamma^{w}_{QH_2^{2+}} \tag{17}$$

$$c^{o}_{QH+} = \frac{K_{a1w} c_{Q\,total} a^{w}_{H+}}{A} \gamma^{o}_{Q} \gamma^{w}_{QH_2^{2+}} \gamma^{w}_{Q} \exp\left(\frac{F(\Delta^{w}_{o}\phi - \Delta^{w}_{o}\phi^{o'}_{QH+})}{RT} \right) \tag{18}$$

$$c^{o}_{QH_2^{2+}} = \frac{c_{Q\,total} [a^{w}_{H+}]^2}{A} \gamma^{w}_{QH+} \gamma^{o}_{Q} \gamma^{w}_{Q} \exp\left(\frac{2F(\Delta^{w}_{o}\phi - \Delta^{w}_{o}\phi^{o'}_{QH_2^{2+}})}{RT} \right) \tag{19}$$

$$a^{o}_{H+} = a^{w}_{H+} \exp\left(\frac{F(\Delta^{w}_{o}\phi - \Delta^{w}_{o}\phi^{o}_{H+})}{RT} \right) \tag{20}$$

where:

$$\begin{aligned} A = & \left[1 + \exp\left(\frac{2F(\Delta^{w}_{o}\phi - \Delta^{w}_{o}\phi^{o'}_{QH_2^{2+}})}{RT} \right) \right] \gamma^{w}_{QH+} \gamma^{o}_{Q} \gamma^{w}_{Q} [a^{w}_{H+}]^2 \\ & + \left[1 + \exp\left(\frac{F(\Delta^{w}_{o}\phi - \Delta^{w}_{o}\phi^{o'}_{QH+})}{RT} \right) \right] \gamma^{w}_{QH_2^{2+}} \gamma^{o}_{Q} \gamma^{w}_{Q} K_{a1w} a^{w}_{H+} \\ & + \gamma^{w}_{QH+} \gamma^{w}_{QH_2^{2+}} K_{a1w} K_{a2w} (\gamma^{w}_{Q} P_Q + \gamma^{o}_{Q}) \end{aligned} \tag{21}$$

The model then allows the evolution of the concentration of each species to be monitored as a function of pH. *Eqn. 20* illustrates that the proton activity is not the same in both phases. The proton activity is much lower in the organic than in the aqueous phase (the exponential factor is always negative in this study), which is due to the physical properties of the solvents, and is represented by this equation.

Moreover, the concentrations of QH_2^{2+} and QH^+ in the aqueous phase can be deduced from experimental data and compared with the above thermodynamic model. Indeed, in cyclic voltammetry, the bulk concentration of a transferring species at the ITIES is related to the recorded peak current by the *Randles-Sevcik* equation, *i.e. Eqn. 22,*

$$i_p = 0.4463 z_i F A c_i^* \left(\frac{z_i F}{RT} \right)^{1/2} D_i^{1/2} v^{1/2} \tag{22}$$

where i_p is the peak current [A], A the interfacial area [cm^2] (in this case $A = 1.3$ cm^2), c_i^* the bulk concentration of species i [mol/cm^3], D_i the diffusion coefficient of i [$cm^2 s^{-1}$], and v the potential scan rate [Vs^{-1}]. In this manner, the accuracy of the experimental results can be compared to the thermodynamic model for confirmation of its validity.

2.4. *Dissociation Constants in the Organic Phase.* The above model can also be used to evalutate the dissociation constants in the organic phase. Similar to *Eqn. 1*, K_{a1o} and K_{a2o} can be defined by *Eqn. 23*. The substitution of equations *Eqns. 6–12* into *23* then yields *Eqns. 24* and *25*.

$$K_{a1o} = \frac{a^{o}_{QH^+} a^{o}_{H^+}}{a^{o}_{QH_2^{2+}}} \quad \text{and} \quad K_{a2o} = \frac{a^{o}_{Q} a^{o}_{H^+}}{a^{o}_{QH^+}} \tag{23}$$

$$K_{a1o} = K_{a1w} \frac{P^{o}_{QH^+} P^{o}_{H^+}}{P^{o}_{QH_2^{2+}}} \tag{24}$$

$$K_{a2o} = K_{a2w} \frac{P_{Q} P^{o}_{H^+}}{P^{o}_{QH^+}} \tag{25}$$

These values are important indicators of pharmacological activity, since they determine the nature and the amount of the various forms of a drug with respect to pH in the aqueous phase and, at the same time, its lipophilicity.

It should be stressed that $P^{o}_{H^+}$, the second exponential term in both *Eqns. 24* and *25*, represents the partitioning of the proton between the water and the organic phase. This parameter has often been neglected in the determination of partition coefficients [19] [20] since the proton activity was considered to be equal in both phases and that the polarization of the interface was also not considered. The comparison between pK_{aw} and pK_{ao} values has then hitherto often been based on this false assumption, because of the inherent difficulty in determining these physical constants.

If the partitioning of the proton is omitted in the calculation, the pK_{ao} values are drastically shifted to lower values. Indeed, with respect to *Eqn. 11*, the pH in the organic phase, pH^{o}, is related to the pH in the aqueous phase, pH^{w}, by *Eqn. 26*. In fact, two different scales should be considered: first, an absolute scale which takes the partition of the proton into account, and second, a 'comparative' scale which substitutes the activity $a^{o}_{H^+}$ by $a^{w}_{H^+}$. The two scales are thus related by *Eqn. 27*.

$$pH^{o} = pH^{w} - \log P_{H^+} = pH^{w} - \log P^{o}_{H^+} - \frac{F \Delta^{w}_{o} \phi}{2.303\, RT} \tag{26}$$

$$pK_{ao} = pK'_{ao} - \log P^{o}_{H^+} \tag{27}$$

Following this definition, if the proton concentration is equal in both phases, the partition coefficient of the proton is set to 1 and the term $\log P^{o}_{H^+}$ disappears in *Eqn. 27*. In this case only, both scales are equivalent. The first scale follows the usual definition of a pK_a, since the pK'_{ao} scale has no direct physical meaning. However, the second scale is commonly used for the evaluation of drug lipophilicity, and this is why it is called 'comparative' in this paper. Indeed, it allows the comparison between partition coefficients and dissociation constants [20].

3. Experimental Part. – Quinidine was supplied by *Sigma* and used without further purification. HNO_3, LiOH, anh. LiCl, Li_2SO_4, KCl, MeOH, $(Me_4N)_2SO_4$, and Bu_4NCl were all supplied by *Fluka;* 1,2-dichloroethane (CH_2ClCH_2Cl) was from *Merck*. Tetrabutylammonium tetrakis(4-chlorophenyl)borate $(Bu_4N)[(C_6H_4Cl)_4B]$ was prepared by metathesis of Bu_4NCl and $K[(C_6H_4Cl)_4B]$ (*Lancaster*) and recrystallized twice from MeOH. All reagents used were anal. grade or purer.

The electrochemical apparatus used was a four-electrode potentiostat, of a design similar to that given in [22], specially made for cyclic-voltammetry experiments. It consisted of an ordinary three-electrode potentiostat and a

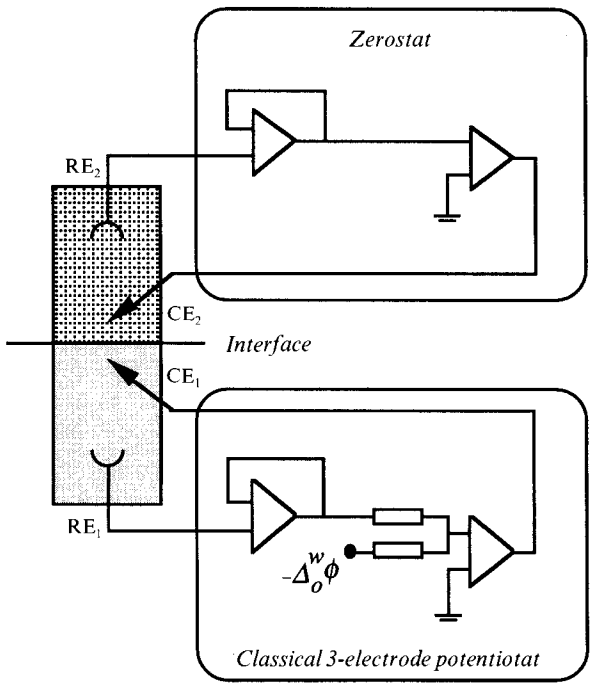

Fig. 3. *Schematic description of the electrical circuit of a potentiostat and of a zerostat.* CE, counter electrode; RE, reference electrode.

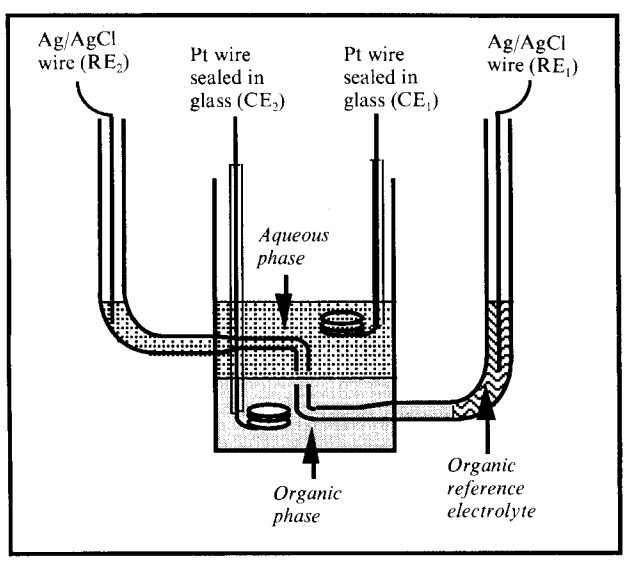

Fig. 4. *Representation of a large ITIES cell for cyclic voltammetry experiments*

homemade zerostat, as schematically illustrated in *Fig. 3*. The reference (RE) and counter electrodes (CE) associated with the org. and aq. phases were connected to the potentiostat and zerostat, resp. The potential waveform was applied to the three-electrode potentiostat, and the zerostat was used to compensate for the ohmic resistance between the two counter electrodes (commonly called *iR* drop compensation), by feedback of a portion of the output signal back into the potentiostat.

The scanning of the applied potential was performed by a waveform generator *PPRI* (*Hi-Tek Instruments*, UK), which was coupled to an *X-Y* recorder (*Bryans Instruments*, UK). The cell used was constructed of glass and was of the design shown in *Fig. 4*. Both the cell and the four-electrode potentiostat were housed in a *Faraday* cage. The cell was kept at r.t. (21 ± 2°) for all experiments.

Quinidine was dissolved in aq. LiCl soln. (base electrolyte) before being poured into the cell. As it dissolved only sparingly, the pH of the aq. soln. was reduced to 4–5 with conc. HNO_3. The pH was then adjusted to the desired value with HNO_3 or LiOH, so as to form a 1 mM quinidine and 10 mM LiCl soln. This constituted the aq. phase, and the volume added to the cell in each experiment was always precisely 1.7 ml so that a constant concentration of quinidine was maintained throughout. The org. phase was a 10 mM $(Bu_4N)[(C_6H_4Cl)_4B]$ soln. in CH_2ClCH_2Cl, and the transfer of quinidine was studied over a pH range of 0 to 8. The cell used for the experiments can be described as:

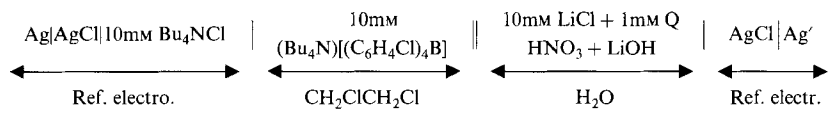

Bu_4N^+-ion-selective electrode

Cell I

In the case of quinidine, the phase in which it is preliminarily dissolved is irrelevant: it can be placed either in H_2O or in CH_2ClCH_2Cl. This was verified experimentally, the results obtained being identical in both cases.

The scan rate was varied between 10 and 100 mVs^{-1}, with both phases unstirred, and *iR* drop compensation was always employed. The org. phase reference electrode was a Bu_4N^+-ion-selective electrode comprising a Ag/AgCl wire immersed in aq. Bu_4NCl soln. Since the formal potential of transfer of the Me_4N^+ ion can be estimated ($\Delta_o^w\phi^{o'}_{Me4N+} = 160$ mV) [23] [24] using an extra-thermodynamic assumption such as the tetraphenylarsonium tetraphenylborate ($(Ph_4As)(Ph_4B)$) scale [25], it was used as reference for the determination of the formal *Gibbs* energy of transfer of the ionized forms of quinidine.

Assuming the validity of *Walden*'s rule [26], the formal potential of transfer of the ion *i* was determined from the voltammograms by application of the simple relation of *Eqn. 28*

$$\Delta_o^w\phi_i^{1/2} - \Delta_o^w\phi_i^{o'} = \Delta_o^w\phi^{1/2}_{Mc4N+} - \Delta_o^w\phi^{o'}_{Me4N+} \tag{28}$$

where $\Delta_o^w\phi_i^{1/2}$ and $\Delta_o^w\phi^{1/2}_{Me4N+}$ are the measured half-wave potentials of the ion *i* and Me_4N^+, resp. The reference was established for each measurement by adding a few drops of 1mM $(Me_4N)_2SO_4$ to the aq. phase. The determination of the formal potential was thus deduced from the voltammograms and from *Eqn. 28*.

In this paper, the transfer of a cation from the aq. to the CH_2ClCH_2Cl phase is defined as a positive current. This relates to the fact that the potential of H_2O with respect to the org. phase is made more positive on the forward scan, a convention valid for all ITIES experiments. It should be stressed at this point that the cyclic voltammetric peaks correspond to a flux of ions across the H_2O/CH_2ClCH_2Cl interface and are in no way redox in nature. Using this definition, the voltammogram of the cation which transfers with a smaller *Gibbs* energy should appear at the less positive potential. On the reverse scan, the transfer of a cation from the CH_2ClCH_2Cl to the aq. phase generates a cathodic current.

The partition coefficient of the neutral form of the quinidine was measured both by a shake-flask method and by *c*entrifugal *p*artition *c*hromatography (CPC) [27] [28]. The values obtained for the log *P* are 2.30 ± 0.23 and 2.50 ± 0.04, resp., and the value of 2.50 was retained for the analysis of the results. The acid-base equilibrium constants of quinidine in the aq. phase were measured with a *Sirius* two-phase titrator [29] and were determined to be: $pK_{a1w} = 4.43 \pm 0.02$ and $pK_{a2w} = 8.66 \pm 0.02$. The values of 4.43 and 8.66 were employed in the thermodynamic model for the calculation of theoretical concentrations.

4. Results and Discussion. – 4.1. *Transfer Behavior of Quinidine Initially Dissolved in the Aqueous Solution.* The dependence of the half-wave potential on pH in the aqueous phase was studied by cyclic voltammetry so as to determine the nature of the transferring

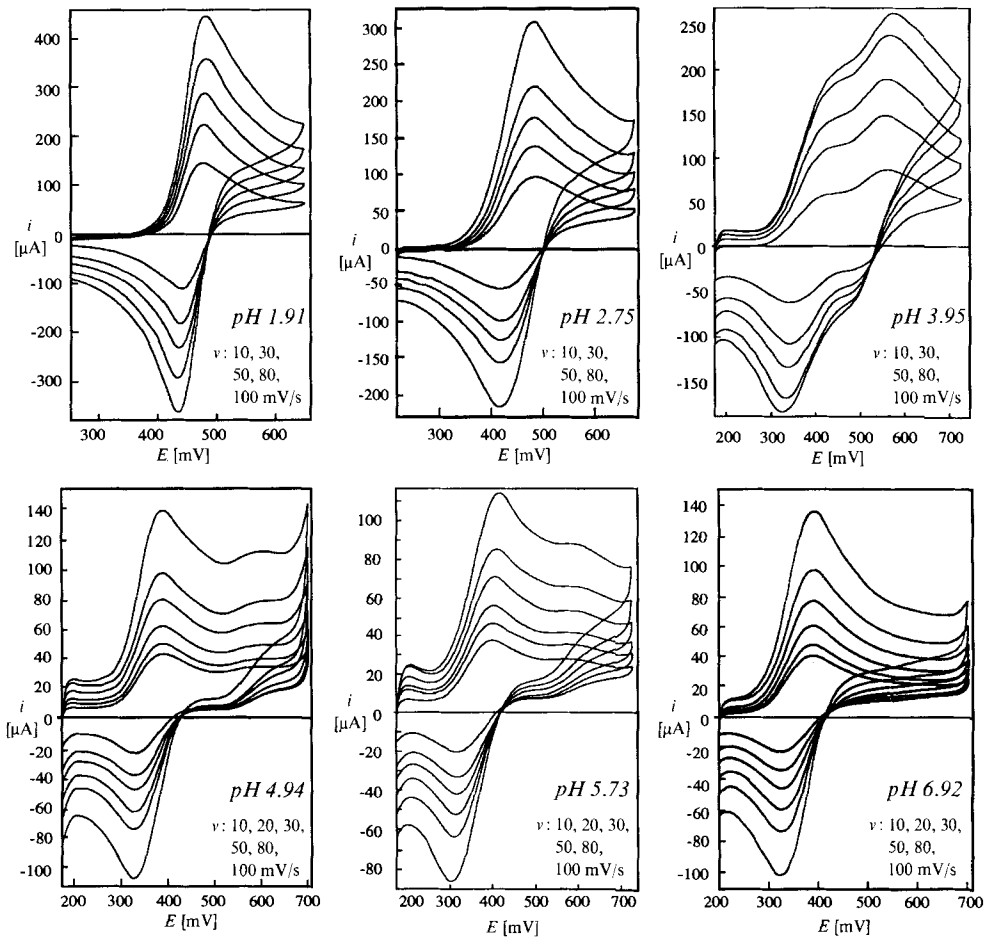

Fig. 5. *Typical cyclic voltammograms of quinidine transfer from H_2O to CH_2ClCH_2Cl.* The direction of the forward scan is from left to right (upper part of the curves), and from right to left for the reverse scan.

species at any given pH. The ionic composition of the quinidine solutions depends on the proton concentration in the aqueous phase, and this is illlustrated in *Fig. 5* which shows several typical voltammograms at different pH values. The structure shown in *Fig. 1* can exist in different forms depending on pH:

a) *From pH 0.5 to 3:* Only one wave is observed. As the potential of the aqueous phase is swept to more positive values, the dication QH_2^{2+} present in this pH range is driven into the organic phase. The shape of the voltammograms indicates that the transfer reaction is reversible and, therefore, diffusion-controlled, implying very fast ion transport across the interfacial region. The transfer is limited by diffusion as shown by the linear dependency between the maximum peak current and the square root of the sweep rate predicted by the *Randles-Sevcik* equation *Eqn. 22.*

The peak-to-peak separation is always *ca.* 30 mV which is the condition for a reversible transfer of a doubly charged ion (since the potential difference between the forward and the reverse peaks is given by the ratio $RT/zF = 59/z$ [mV]). Therefore, this peak can be attributed conclusively to QH_2^{2+}.

b) *From pH 3 to 6:* A second peak appears at a less positive potential than the former wave. The first peak observed when the potential is swept to more positive values corresponds to the transfer of QH^+ from H_2O to the organic phase. This shows that the monovalent cation has a more negative formal transfer potential than that of the divalent cation. Thus it has a smaller *Gibbs* energy, can more easily cross the H_2O/CH_2ClCH_2Cl interface, and can be assumed to be more lipophilic than the doubly charged ion.

As pK_{a1w} is 4.43, the concentration of QH^+ increases over this range of pH, while that of QH_2^{2+} diminishes. This is confirmed by the voltammograms, since the peak height of the QH^+ wave increases progressively with pH, while that of QH_2^{2+} decreases.

c) *From pH 6 to 7.5:* The first peak disappears completely, and only one wave is observed. With respect to the acid-base equilibrium in the aqueous phase, the only charged species present at such pH values is QH^+, and the peak observed can conclusively be attributed to this cation. Despite experimental errors, the peak-to-peak separation varies very little around 60 mV, which confirms the transfer to be that of a singly charged ion. Furthermore, the fact that a single wave is also observed in this pH range validates the hypothesis of the transfer of QH_2^{2+} between pH 0 and 3 and of both cations between pH 3 and 6.

It should be noted that with increasing pH, the reverse peak of QH_2^{2+} becomes less and less pronounced relative to the forward peak. Furthermore, the voltammograms in *Fig. 5* show that the reverse peak current of QH^+ is slightly greater than expected. This can be explained by the fact that the doubly charged quinidine is much more hydrophilic than the singly charged species. Consequently, when QH_2^{2+} enters the reaction layer of the organic phase, it is instantaneously deprotonated in order to gain stability. This justifies the separation of the phases into a bulk and a reaction layer, as described in the thermodynamic scheme of *Fig. 2*.

4.2. *Formal* Gibbs *Free Energy of Transfer.* The transfer of quinidine was studied over the pH domain of 0 to 7.5, and the pH dependence of the formal potential is shown in *Fig. 6* where the different pH ranges decribed above can be easily identified.

By applying *Eqn. 28,* a mean value of $\Delta_o^w\Phi^{o'}$ can be determined for both doubly and singly charged quinidine which yields:

$$\Delta_o^w\phi^{o'}_{QH_2^{2+}} = 162 \pm 4 \text{ mV and } \Delta_o^w\phi^{o'}_{QH^+} = 80 \pm 9 \text{ mV}$$

The formal *Gibbs* free energies of transfer of both QH^+ and QH_2^{2+} are then directly deduced from their definition (*Eqn. 5*). On the (Ph_4As) (Ph_4B) scale:

$$\Delta G^{o',w\to o}_{tr,QH^+} = zF\cdot\Delta_o^w\phi^{o'}_{QH^+} = 7.7 \pm 0.9 \text{ kJ mol}^{-1}$$

$$\Delta G^{o',w\to o}_{tr,QH_2^{2+}} = zF\cdot\Delta_o^w\phi^{o'}_{QH_2^{2+}} = 31.2 \pm 0.7 \text{ kJ mol}^{-1}$$

With these two values, we can calculate the ratio of the concentration of the ionic species as a function of the *Galvani* potential difference. Indeed, using *Eqns. 5, 7,* and *9,* we have obtain *Eqns. 29* and *30.*

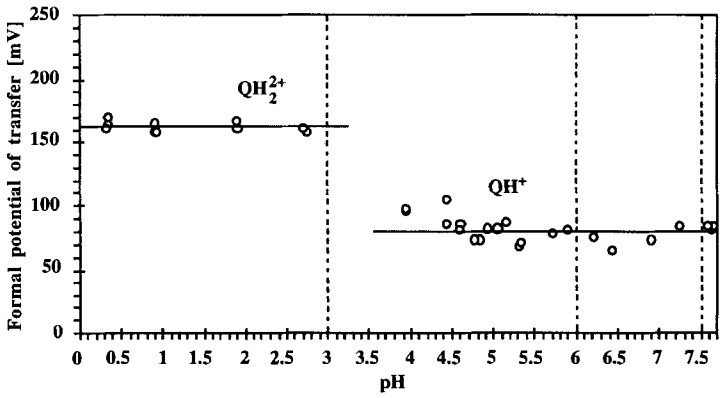

Fig. 6. *Relationships between the formal potential of transfer and pH in the aqueous phase*

$$\log\left[\frac{c^{o}_{QH^+}}{c^{w}_{QH^+}}\right] = \frac{F\Delta^{w}_{o}\phi}{2.303\,RT} - \frac{\Delta G^{o',\,w\to o}_{tr,\,QH^+}}{2.303\,RT} = -1.37 + \frac{\Delta^{w}_{o}\phi}{0.059} \tag{29}$$

$$\log\left[\frac{c^{o}_{QH_2^{2+}}}{c^{w}_{QH_2^{2+}}}\right] = \frac{F\Delta^{w}_{o}\phi}{2.303\,RT} - \frac{\Delta G^{o',\,w\to o}_{tr,\,QH_2^{2+}}}{2.303\,RT} = -5.54 + \frac{\Delta^{w}_{o}\phi}{0.059} \tag{30}$$

These values allow us to determine the standard partition coefficients defined by *Eqns. 8* and *10*. In a first approximation, we can neglect in *Eqn. 5* the term involving the ratio of the activity coefficients so that we have:

$$\log P^{o}_{QH^+} = -1.37 \pm 0.16 \quad \text{and} \quad \log P^{o}_{QH_2^{2+}} = -5.54 \pm 0.12$$

These values confirm that the singly charged quinidine needs less energy to cross the interface than the doubly charged quinidine and emphasizes its greater lipophilicity.

4.3. *Dissociation Constants in the Organic Phase.* The thermodynamic model presented in *Sect. 2* allows evaluation of the dissociation constants in the organic phase (*Eqns. 24* and *25*). These two relationships yield in the present case:

$$pK_{a1o} = pK_{a1w} + \log P^{o}_{QH_2^{2+}} - \log P^{o}_{QH^+} - \log P^{o}_{H^+} = 9.66 \pm 0.21$$

$$pK_{a2o} = pK_{a2w} + \log P^{o}_{QH^+} - \log P^{o}_{H^+} - \log P_{Q} = 14.20 \pm 0.16$$

These values are much larger than those for the aqueous phase (4.43 and 8.66, resp.). The activity of the proton in the organic phase, $a^{o}_{H^+}$, is always very small, so that the protonation equilibria in the organic phase are constantly shifted so as to favor the species of lower charge. Moreover, because of the low value of $a^{o}_{H^+}$, the pK_{ao} values are drastically displaced to higher values. As mentioned previously, this explains why they do not correspond to the data commonly found in the literature [19] [20].

Nevertheless, as the formal potential of transfer of proton is equal to 549 mV [30] and as the equilibrium between both phases is established at an applied *Galvani* potential of zero, *Eqn. 12* yields in a first approximation neglecting the ratio of the activity coefficient:

$$\log P^{o}_{H^+} = -9.41$$

In this manner, when the partitioning of the proton is neglected, both pK_{ao} values decrease by 9.41 units, yielding on the comparative scale:

$$pK'_{a1o} = 0.26 \pm 0.21 \quad \text{and} \quad pK'_{a2o} = 4.79 \pm 0.16$$

These two values are displaced by about four units with respect to their corresponding pK_{aw} values. This means that quinidine has a smaller affinity for the proton and, consequently, that it is less basic in CH_2ClCH_2Cl than in H_2O. This is due to the lack of H-bonds in CH_2ClCH_2Cl which prevents the stabilization of the ionized form of the quinidine and favors the presence of the neutral species.

4.4. *Validity of the Thermodynamic Model.* 4.4.1. *Determination of the Diffusion Coefficient of* QH_2^{2+}. With respect to the dissociation equilibria, and from the above experimental results, only QH_2^{2+} is present at very low pH, and it is completely retained in the aqueous phase. As described in the experimental part (see *Cell I*), the total amount of quinidine is always known. Consequently, at very low pH, the quinidine concentration in the aqueous phase is fixed at the value of 1 mM. By plotting the maximum peak current as a function of the square root of the scan speed, the diffusion coefficient of QH_2^{2+} can then be determined by application of the *Randles-Sevcik* relation (*Eqn. 22*), as shown in *Fig. 7*.

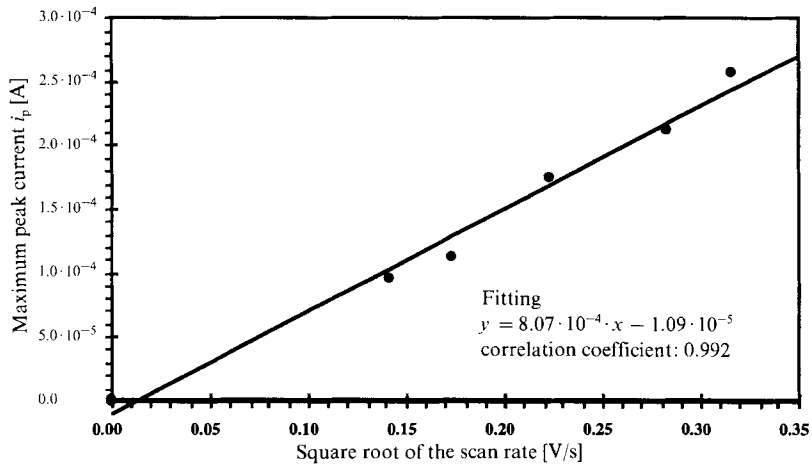

Fig. 7. *Relationship between maximum peak current and square root of the scan speed to allow determination of the diffusion coefficient of quinidine*

Thus, $D_{QH_2^{2+}} = 1.23\ 10^{-6} \pm 0.04\ 10^{-6}\ cm^2\ s^{-1}$. This value is then used for the evaluation of the aqueous bulk concentration of quinidine as a function of the pH, which provides the experimental data found in *Fig. 11* (see below) and a comparison with the thermodynamic model.

4.4.2. *Theoretical Concentration Profiles.* Using the values of the formal transfer potential of both QH^+ and QH_2^{2+} given above, that of the partition coefficient, and also the equilibrium constants of the quinidine given in the *Exper. Part*, it is straightforward to solve the system described by *Eqns. 6–13* taking all activity coefficients as unity. The dependence of the various quinidine species in the aqueous phase and in the organic phase

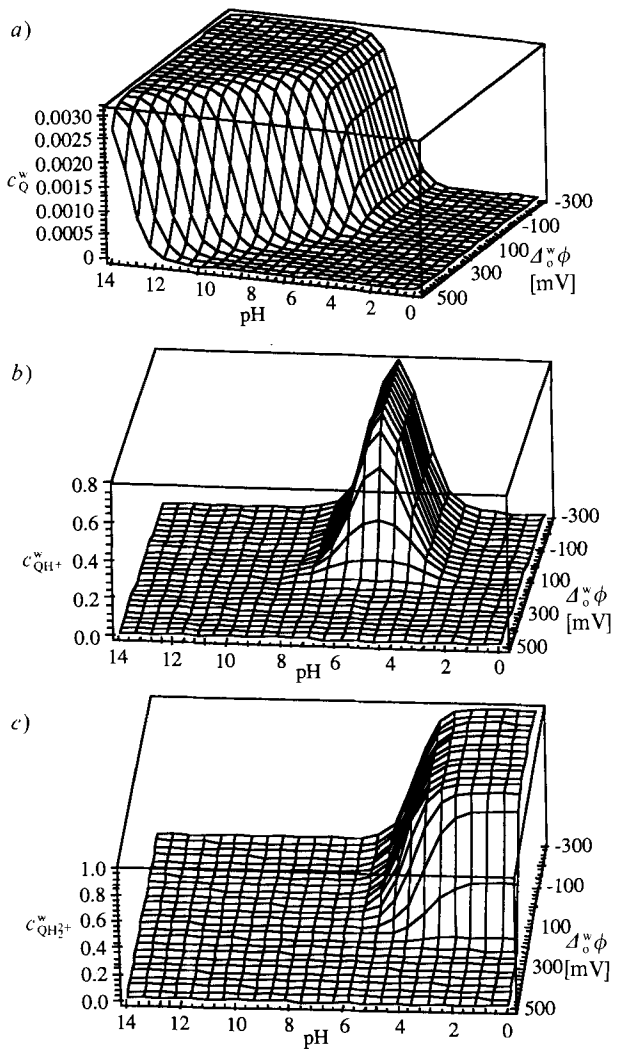

Fig. 8. *Theoretical concentration profiles in the aqueous phase for* a) *neutral quinidine,* b) *singly charged quinidine, and* c) *doubly charged quinidine*

on pH and applied *Galvani* potential are illustrated in *Figs. 8* and *9*, respectively. These figures clearly demonstrate that the applied potential is an important driving force which pushes all of the species in the aqueous phase into the organic phase: at a given pH, the concentrations of c^w_Q, $c^w_{QH^+}$, and $c^w_{QH_2^{2+}}$ diminish with the applied potential, since, at the same time, the concentrations of singly or doubly charged quinidine in the organic phase increase. This is in good agreement with the high value of P and with the fact that the aqueous phase is made more positive with respect to the organic phase when the applied potential is increased. Consequently, the protonation equilibria in both phases vary with the applied potential, although the dissociation constants remain unchanged.

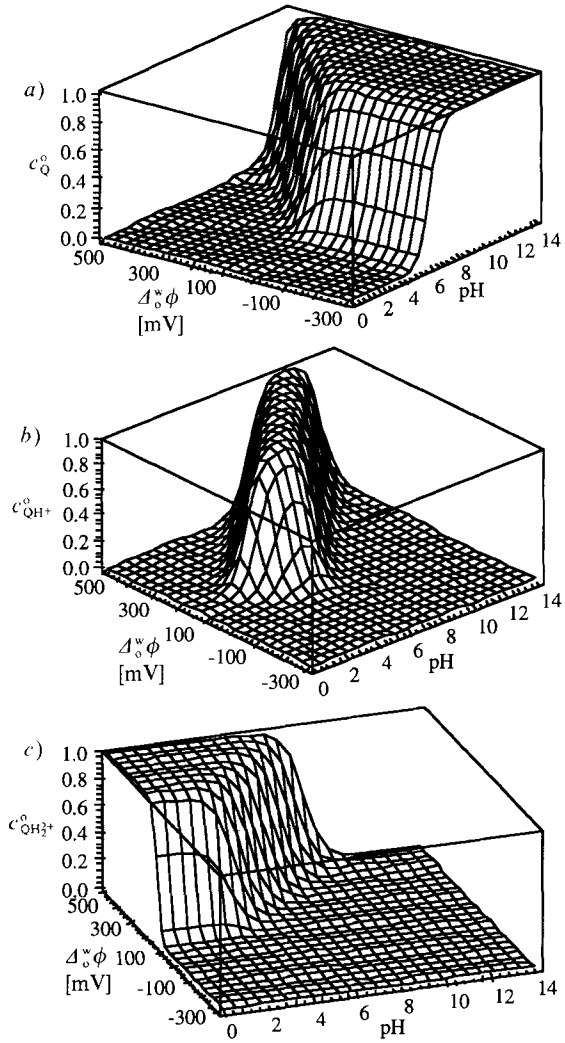

Fig. 9. *Theoretical concentration profiles in the organic phase for* a) *neutral quinidine*, b) *singly charged quinidine, and* c) *doubly charged quinidine*

Moreover, at the beginning of each experiment, the applied potential is set to zero. The equilibria between all the different species in both H_2O and CH_2ClCH_2Cl are thus established at such a potential. Consequently, the bulk concentrations are determined by following the above three dimensional profiles with $\Delta^{w}_{o}\Phi$ fixed at a value of 0 mV. In this manner, one can calculate the dependence of the concentrations on the pH in the aqueous phase, as represented in *Fig. 10.*

4.4.3. *Comparison with Experimental Results.* The quality of the thermodynamic model can be verified by comparison with the concentrations deduced from the experimental results for the doubly charged quinidine which is illustrated in *Fig. 11.* When the

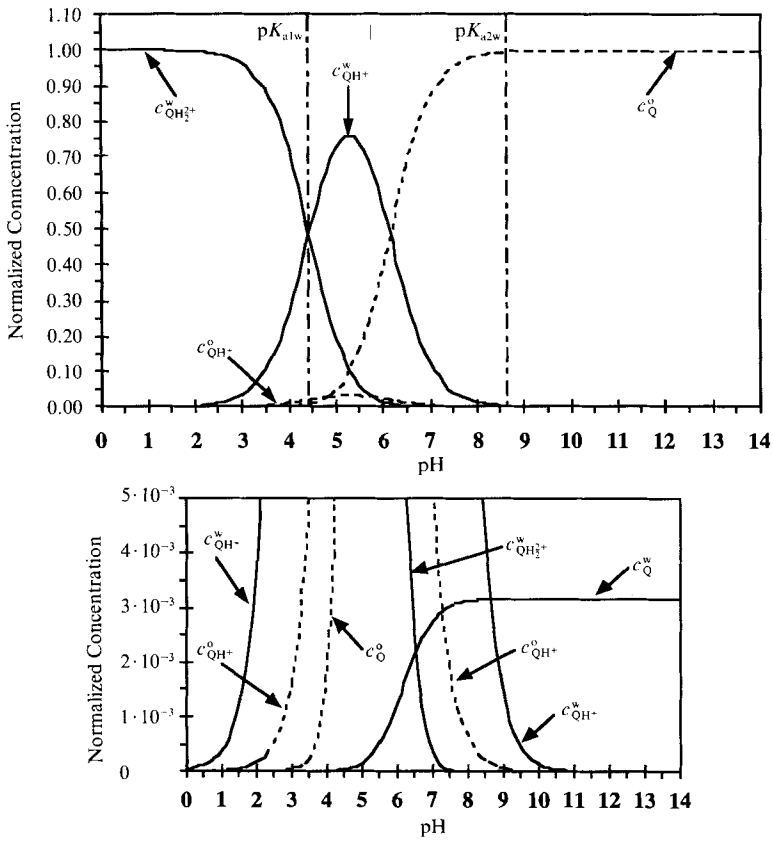

Fig. 10. *Theoretical concentration profiles in both phases of all forms of quinidine as a function of the pH in the aqueous phase.* $c^o_{QH_2^{2+}}$ does not appear on this graph, since this concentration is negligible.

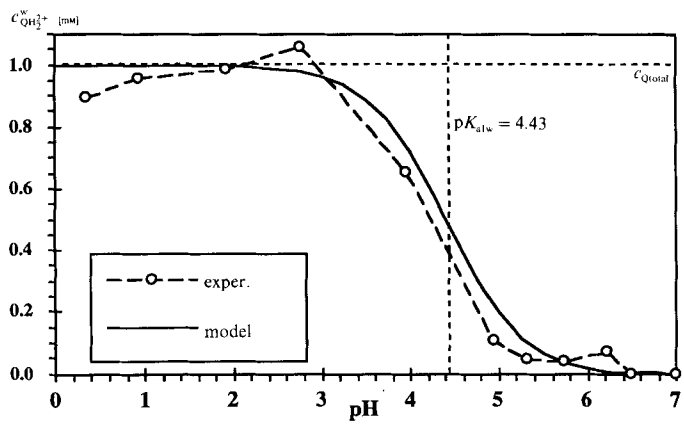

Fig. 11. *Concentration profile of the doubly charged quinidine: comparison between experimental and theoretical results*

pH is equal to pK_{a1w}, the concentration of the doubly charged quinidine should be 0.5 mM according to the protonation equilibria of the aqueous phase. However, as the water is in contact with the organic phase, and since the partition coefficient of quinidine is high, the concentration profile of QH_2^{2+} is displaced towards the left. So, at pH 4.43, the concentration of QH_2^{2+} is 0.48 mM when calculated with our model, which suggests that the concentration of the doubly charged quinidine diminishes more rapidly with pH than previously believed.

The experimental results confirm this behavior despite the difference in ionic strength and experimental errors. This explains the differences between the experimental results and the model (*Fig. 11*) and also proves its validity.

5. Conclusion. – This study shows that both singly and doubly charged quinidine can transfer across the H_2O/CH_2ClCH_2Cl interface. At pH values higher than 6, a single transfer wave is observed which is due to singly charged quinidine. The parameters evaluated from the cyclic voltammetric experiments are summarized in the *Table*.

Table. *Summary of the Main Parameters Established from the Experiments*

	$\Delta_o^w\phi^{o'}$ [mV]	$\Delta_o^w G_{tr,i}^{o',w\to o}$ [kJ mol^{-1}]	log P_i[a])	pK_{aw}	pK_{ao}	pK'_{ao}
QH_2^{2+}	162 ± 4	31.2 ± 0.7	−5.54 ± 0.12	4.43 ± 0.02	9.66 ± 0.21	0.26 ± 0.21
QH^+	80 ± 9	7.7 ± 0.9	−1.37 ± 0.16	8.66 ± 0.02	14.20 ± 0.16	4.79 ± 0.16

[a]) log P_Q is 2.5 ± 0.04 and was measured by CPC.

The thermodynamic model described in this paper fits these results. It also allows the calculation of the concentration of all the different species present in the aqueous and organic phases. A direct result of this is the possibility to evaluate the equilibrium constants in the organic phase. The determined values of pK_a in the organic phase (see *Table*) are much greater than in the aqueous phase because of the partitioning of the proton. If this partitioning is omitted in the calculation, another scale can be established, where the new pK_{ao} values, pK'_{ao}, are decreased by 9.41 units.

The new approach described here leads to an improved understanding of the physicochemical molecular mechanisms of passive transfer of organic ions and overcomes the main limitation of the commonly accepted hypothesis, *i.e.* the neglect of the partitioning of ionic species.

The electrochemical technique and the thermodynamic modelling derived here will be utilized in further work to describe the distribution behavior of ionic drugs and their lipophilicity, so as to determine how drug absorption, distribution, storage, and excretion can be evaluated by their transfer mechanisms.

P.-A. C., H. G., and *B. T.* are grateful for the support by the *Swiss National Science Foundation*.

REFERENCES

[1] V. S. Markin, A. G. Volkov, *Electrochim. Acta* **1989,** *34,* 93.
[2] M. Senda, T. Kakiuchi, T. Osakai, *Electrochim. Acta* **1991,** *36,* 253.
[3] J. Koryta, *Selective Electrode Rev.* **1991,** *13,* 133.
[4] H. H. Girault, 'Charge Transfer across Liquid/Liquid Interfaces', in 'Modern Aspects of Electrochemistry', Eds. J. O'M. Bockris, B. Conway, and R. White, Plenum Press, New York, 1993, Vol. 25, pp. 1–62.
[5] J. Koryta, M. Skalicky, *J. Electroanal. Chem.* **1987,** *229,* 265.
[6] H. H. Girault, D. J. Schiffrin, 'Electrochemistry of Liquid/Liquid Interfaces', in 'Electroanalytical Chemistry', Ed. A. J. Bard, Marcel Dekker, New York–Basel, 1989, Vol. 15, pp. 1–141.
[7] E. Wang, H. Ji, *Electroanalysis* **1989,** *1,* 75.
[8] T. Solomon, *J. Electroanal. Chem.* **1991,** *313,* 29.
[9] Y. Shao, S. N. Tan, V. Devaud, H. H. Girault, *J. Chem. Soc., Faraday Trans.* **1993,** *89,* 4307.
[10] M. D. Osborne, H. H. Girault, *Electroanalysis* **1995,** *7,* 425.
[11] J. D. Fenstermacher, 'Drug Transfer across the Blood-Brain Barrier', in 'Topics in Pharmaceutical Sciences 1983', Eds. D. D. Breimer and P. Speiser, Elsevier, Amsterdam, 1983, pp. 143–154.
[12] C. J. Alcorn, R. J. Simpson, D. E. Leahy, T. J. Peters, *Biochem. Pharmacol.* **1993,** *45,* 1775.
[13] J. B. M. M. van Bree, A. G. de Boer, M. Danhof, D. D. B. Breimer, *Pharmacy World Science* **1993,** *15,* 2.
[14] M. G. Davis, C. N. Manners, D. W. Payling, D. A. Smith, C. A. Wilson, *J. Pharm. Sci.* **1984,** *73,* 949.
[15] W. A. Banks, A. J. Kastin, *Brain Res. Bull.* **1985,** *15,* 287.
[16] D. A. Smith, K. Brown, M. G. Neale, *Drug Metab. Rev.* **1986,** *16,* 365.
[17] W. Martha, 'The Merck Index, an Encyclopedia of Chemicals, Drugs, and Biologicals', Merck & Co., Rahway, USA, 1983, pp. 1282.
[18] R. Doherty, W. R. Benson, M. Maienthal, J. Stewart, *J. Pharm. Sci.* **1978,** *67,* 1698.
[19] R. S. Tsai, N. El Tayar, P.-A. Carrupt, B. Testa, *Int. J. Pharm.* **1992,** *80,* 39.
[20] R. A. Scherrer, S. L. Crooks, 'Titration in Water-Saturated Octanol: a Guide to Partition Coefficients of Ion Pairs and Receptor-Site Interaction', in 'QSAR: Quantitative Structure-Activity Relationships in Drug Design, Ed. A. R. Liss, Fauchère, New York, 1989, pp. 59–62.
[21] J. Barthel, H. J. Gores, G. Schmeer, R. Wachter, 'Non-Aqueous Electrolyte Solutions in Chemistry and Modern Technology', in 'Topics in Current Chemistry', Ed. D. L. Boschke, Springer Verlag, Berlin, 1983, Vol. 111, pp. 33–144.
[22] Z. Samec, J. Weber, V. Marecek, *J. Electroanal. Chem.* **1979,** *100,* 841.
[23] T. Wandlowski, V. Marecek, Z. Samec, *Electrochim. Acta* **1990,** *35,* 1173.
[24] Y. Shao, 'Ion Transfer across Liquid/Liquid Interfaces', Ph.D. Thesis, University of Edinburgh, 1991, pp. 187.
[25] E. Grunwald, G. Baughman, G. Kohnstam, *J. Am. Chem. Soc.* **1960,** *82,* 5801.
[26] A. J. Bard, L. R. Faulkner, 'Electrochemical Methods: Fundamentals and Applications', J. Wiley & Sons, New York, 1980, pp. 152–154.
[27] N. El Tayar, R.-S. Tsai, P. Vallat, C. Altomare, B. Testa, *J. Chromatogr.* **1991,** *556,* 181.
[28] R.-S. Tsai, P.-A. Carrupt, B. Testa, 'Measurement of Partition Coefficients Using Centrifugal Partition Chromatography', in 'Modern Countercurrent Chromatography', Eds. W. D. Conway and R. J. Petroski, American Chemical Society, Washington, DC, 1995, Vol. 593, pp. 143–154.
[29] A. Avdeef, *J. Pharm. Sci.* **1993,** *82,* 1.
[30] A. Sabela, V. Marecek, Z. Samec, R. Fuoco, *Electrochim. Acta* **1992,** *37,* 231.